Journal of Magnetism and Magnetic Materials 553 (2022) 169266

Contents lists available at ScienceDirect

Journal of Magnetism and Magnetic Materials

journal homepage: www.elsevier.com/locate/jmmm

Magnetic annealing of extruded thermoplastic magnetic elastomers for 3D-Printing via FDM

Nathan A. Fischer [a], Alex L. Robinson [a], Thomas J. Lee [a], Thomas M. Calascione [a], Lucas Koerner [b], Brittany B. Nelson-Cheeseman [a,*]

[a] Mechanical Engineering, University of St. Thomas, St. Paul, MN, USA
[b] Electrical & Computer Engineering, University of St. Thomas, St. Paul, MN, USA

ARTICLE INFO

Keywords:
Magnetorheological elastomer
Extrusion
Magnetic annealing
Magnetic properties
Magnetoactive properties
Fused Deposition Modeling (FDM)

ABSTRACT

Magnetorheological elastomers (MREs) are magnetoactive smart materials that exhibit mechanical deformation in the presence of magnetic fields. The greatest performance in these materials has been seen from magnetic annealing, which creates high internal anisotropy. This work studies how different magnetic annealing setups (no field, uniform field, and non-uniform field) can be applied to thermoplastic MRE extrusion geometries and how each setup affects the resulting magnetic and magnetoactive properties. The uniform field resulted in an increase of both magnetic anisotropy and magnetoactive performance when compared to no field (but was difficult to make samples with). The non-uniform magnetic annealing setup resulted in similar magnetic properties but decreased magnetoactive performance when compared to the no field samples likely due to interference with the naturally occurring anisotropy that results from extrusion flow. This work demonstrates that certain magnetic annealing setups can be applied to extrusion geometries for increased anisotropy effects resulting in greater magnetoactive response compared to no magnetic annealing, while others can lead to a decrease in anisotropy and less magnetoactive response.

1. Introduction

Smart materials are desired for their unique responsive properties allowing them to be used in advanced applications. For example, magnetorheological composites mechanically deform in response to an applied magnetic field. Magnetorheological elastomers (MRE) are a subset that exhibit large deformation strains which allow for a greater response. Some applications for these materials are sensors, actuators, dampeners, and soft robotics [1]. As with all composites, their properties can be influenced by the component material types and through manipulating internal structures.

Anisotropy is created when the structure of a material has alignment in certain directions; this then creates different properties along different directions within the material. Within magnetically responsive materials, it has been shown that increasing the anisotropy of the magnetic properties also increases their overall performance [2]. A common technique for increasing magnetic anisotropy is magnetic annealing. In magnetic polymer composites, magnetic annealing involves applying a magnetic field in the axial orientation while the polymer matrix is partially viscous to align the internal particulate. While applying the magnetic field, the matrix is cooled or cured to trap the particulate in place resulting in increased anisotropy. For this process both uniform and non-uniform magnetic fields can be used. With geometrically anisotropic particulate, the magnetic field creates an orientation effect as particles rotate with respect to the applied field. Within all particulate types, the magnetic field polarizes internal particulate and can form chains while still allowing for orientation effects from geometrically anisotropic particulate to occur. By differing the field type used, the orientation of particulate and the length and continuity of these chains are affected and result in different amounts of anisotropy [3–5].

Just as increased anisotropy from magnetic annealing has shown to increase performance in magnetorheological elastomers, it is hypothesized that the increased internal anisotropy from Fused Deposition Modeling (FDM) could also lead to increased MRE performance [6,7]. FDM is a 3D printing technique that creates internal *meso*-structural anisotropy by extruding a viscous material in 1D lines to form 2D planes that build up to a 3D part. Alignment of the magnetic particulate *via* this process would further bolster the anisotropy and, likely, the performance of the printed part. Axial magnetic annealing during the 3D

* Corresponding author.

https://doi.org/10.1016/j.jmmm.2022.169266
Received 28 May 2021; Received in revised form 6 February 2022; Accepted 10 March 2022
Available online 12 March 2022

printing extrusion process have necessitated specialized 3D printers or specialized materials, or magnetic ink [8–10]. Creation of thermoplastic magnetic filament material for FDM and the use of magnetic annealing has been explored but requires further investigation [11–13]. Magnetic annealing of filament before and during 3D printing has been demonstrated through the use of embedded permanent magnets during the extrusion process but do not explore using varied magnetic field profiles to encourage greater anisotropy effects [8,11]. This work seeks to use tailored magnetic field profiles in axial magnetic annealing of thermoplastic magnetic filament for FDM to provide an approach that is much more accessible and may lead to greater control of anisotropy than other magnetic annealing processes.

This work investigates two fully characterized magnetic fields for axial magnetic annealing (uniform and non-uniform) in order to understand how each affects the anisotropy and properties of the resulting extruded thermoplastic composite. The magnetic and magnetoactive properties of the extruded filaments are tested and compared with filament extruded under zero applied magnetic field. It was found that the magnetic annealing field presence and profile does affect the magnetic and magnetoactive properties of FDM extruded thermoplastic elastomers.

2. Methods

Stock composite material was made via solvent casting [14] whereby Ninjaflex^{TM} (a thermoplastic elastomer matrix material) [15] is integrated with 15 vol% iron particulate. The particulate is water atomized iron powder of sizing 100 mesh (<150 μm) and irregularly shaped. Using a Filabot EX2, the solvent cast composite was extruded into 2 mm filament. Filament was extruded at 186 °C for each sample type using a 2 mm diameter nozzle and extruding at a rate of 30 in. per minute. After the filament exited the extrusion nozzle, it was cooled to room temperature (21 °C) *via* air jets (Fig. 1) and wound onto a spool. The air jets were focused to a point 6 cm past the extruder nozzle along the path that the filament travels after extrusion.

The magnetically annealed samples undergo a similar process but also pass through a permanent magnet (NdFeB) setup immediately after extrusion (while still partially viscous). Air jets cool the filament inside the permanent magnet setup to trap particulate in place and maintain any rotational or chaining effects originating from the magnetic field. This in-line magnetic annealing aspect allows for the filament geometry to be maintained. Three different magnetic field configurations were explored: no applied field consisting of 0 magnets per stack (0 M), a uniform axial applied field consisting of 5 magnets per stack (5 M), and a nonuniform axial applied field consisting of 3 magnets per stack (3 M).

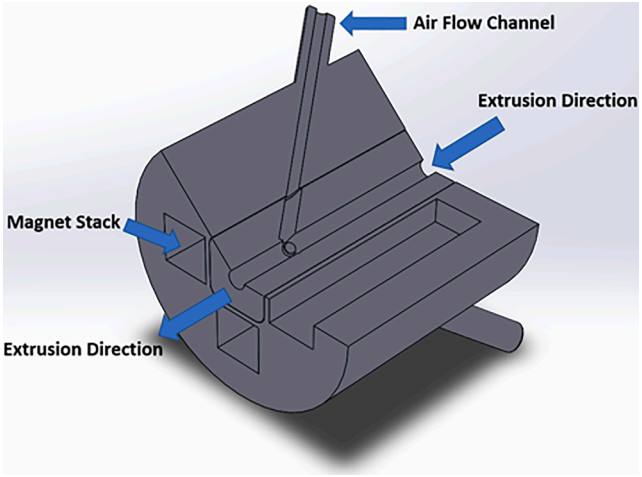

Fig. 1. Sectioned 3D model of the magnet holder cut to highlight magnet positions (x4) and air flow channels (x4).

Both the uniform and nonuniform fields were created by placing linear magnet stacks at 25.4 mm (1in) radially from the center of the nozzle at four different locations with each stack aligned parallel to the extrusion direction, shown in Fig. 1. Fig. 2 shows that the uniform (5 M) field stacks were made up of five contiguous 12.7 mm NdFeB cube shaped magnets, while the nonuniform (3 M) field magnet-stacks were each made up of three isolated 12.7 mm NdFeB cube shaped magnets each separated by a cylindrical low carbon steel spacer of a similar size, that acts as a saturated magnet. Both total stacks were of similar length 63.5 mm and were orientated with their south poles at the entrance of permanent magnet setup and their north poles at the exit.

In order to characterize the magnetic field profiles of the 3 M and 5 M setups, a Bell 7030 gaussmeter and a Tektronix probe with XYZ direction and magnitude capabilities were used. The probe was mounted onto a 3D printer head and then scanned stepwise every 3 mm in an orthogonal mesh around and within each magnetic annealing setup. Fig. 2C has an average value of 97.8mT with a standard deviation of 10.06mT. Comparing this to Fig. 2D which has an average value of 86.23mT and standard deviation of 13.83mT, it shows that the 5 M magnet setup has a field with a greater overall strength and less deviation in magnitude. Both measured magnetic field profiles exhibit less than a 6° angle off the central axis throughout the entire field profile, indicating the largely axial nature of the field direction in both. This small deviation is likely due to defects within the magnets and interfering magnetic fields. This may slightly disrupt anisotropy from rotational effects but should have little overall effect on anisotropy. The standard deviation of the magnetic field shows the relative amount of oscillation between different field types. A smaller standard deviation of both the magnitude and direction of the field indicates that the particulate experiences a more constant field profile as it travels through the setup as it cools. This should lead to more robust chaining particulate effects from the magnetic annealing, leading to greater magnetic anisotropy and magnetoactive deflection. This can be used to tailor magnetic fields for either stronger magnetic moments or more instances of magnetic moments to create anisotropy through chaining or orientation effects on internal particulate respectively. The 5 M magnet setup creates a more uniform axial magnetic field due to having two flux concentrations at the poles creating a single intermediate minimum. The 3 M magnet setup creates three concentrated areas of flux through the use of spacers resulting in two minima along the axis of extrusion. Both setups also have a dominant axial component to the field direction along the extrusion direction along the central axis of each setup. Between the two setups, 5 M has a greater average magnitude and less oscillation in the magnitude of the field along the central axis.

To understand the effect of the magnetic annealing setups, the magnetic and magnetoactive properties of the resulting extruded filaments were measured and compared. Six samples from each sample type were used for magnetoactive testing and three samples of each type were used for magnetic testing. Samples with notable defects and significant diameter inconsistency were removed from the sample pool. The magnetic properties of extruded filament samples with a length of 12 mm were recorded using a vibrating sample magnetometer (VSM) via +/- 1 T hysteresis loops with the applied field both parallel (axial) and perpendicular (transverse) to the filament axis. The magnetoactive properties were measured by hanging filament samples with a length of 50 mm vertically between two large electromagnets and then varying the applied field. The maximum applied field was 0.4 T as it is the maximum field of the system. The resulting sample deflections for various applied magnetic fields were recorded *via* image capture. The measured angles of deflection relative to the applied magnetic fields were plotted to identify magnetoactive trends. Each sample had an initial angle of deflection of 0°at 0 T.

3. Results and discussion

The axial and transverse hysteresis loops of the 0 M, 3 M and 5 M

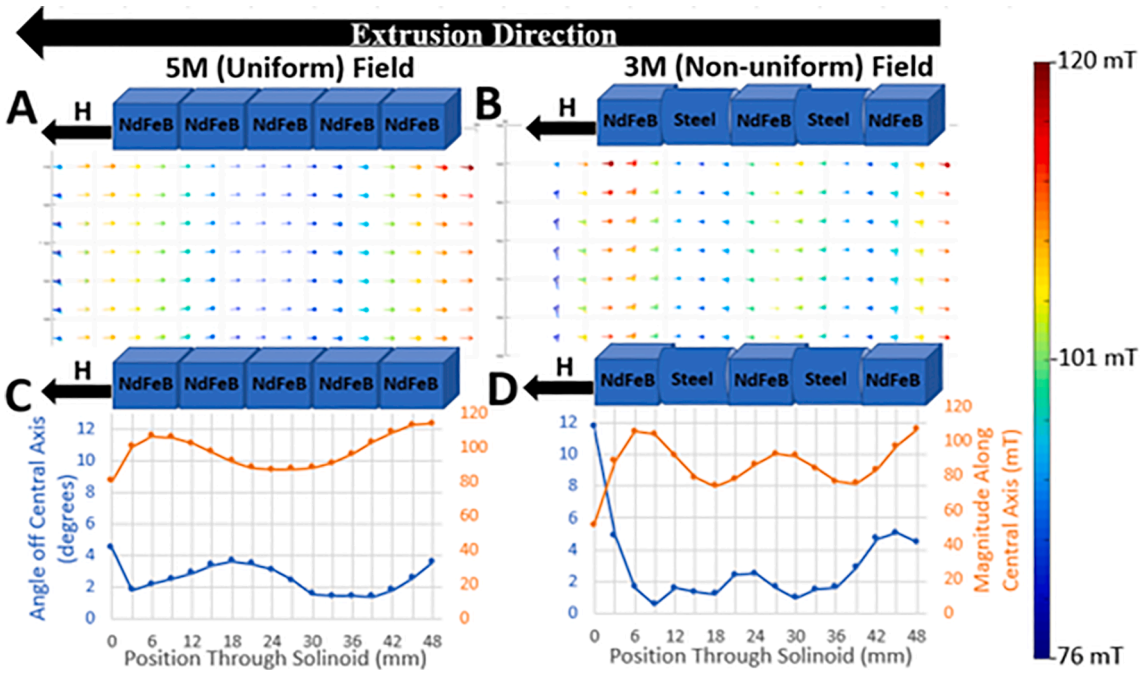

Fig. 2. (A,B) Magnetic field characterizations with illustrations of magnet stacks used. Vector magnitude is denoted by the color scale on the righthand side with red being strongest rather than vector size. This vector field is three dimensional, but the central slice is projected onto the 2D plane for viewing the section of magnetic field used in magnetic annealing. (C,D) Change in vector angle as a function of position and corresponding field magnitude as a function of position for 5 M and 3 M, respectively. (For interpretation of the references to color in this figure legend, the reader is referred to the web version of this article.)

filaments are shown in Fig. 3. The graph uses magnetization normalized by maximum magnetization to be able to compare the magnetic moment between the sample types. To further highlight changes in magnetic moments between the samples, subtraction of the 5 M and 3 M loops from the 0 M loop was used (Fig. 3). The 0 M sample act as a baseline for relative anisotropy when comparing samples processed under magnetic field conditions. In the axial (parallel) applied field, the 5 M samples show an increased rate of magnetization over applied field, likely dominated by macroscopic shape anisotropy effects. 3 M samples however have a small initial increase in its rate of magnetization then become weaker than the 0 M samples. This indicates that 5 M magnetic annealing setups show increased magnetic anisotropy compared to 3 M samples and samples with no magnetic annealing. In the transverse (perpendicular) applied field, the 3 M samples showed the greatest amount of magnetic anisotropy and the 5 M samples showed the least. This indicates that the 5 M magnetic annealing setup had a greater orientation effect along the extrusion direction as its magnetic anisotropy along the transverse axis decreased when compared to the 3 M and 0 M samples.

The fact that the 3 M samples have greater magnetic anisotropy in the transverse direction when compared to the 0 M samples and indicates that the 3 M magnetic annealing setup may have interfered with inherent magnetic alignment created by drag forces in the extrusion process. This caused significant effects as the 3 M magnetic field profile does not create an increase in magnetic anisotropy when compared to 0 M samples. In the future, reducing the drag forces present during extrusion could reduce natural anisotropy and allow rotational effects to operate unimpeded [16,17]. The results between 3 M and 5 M show that

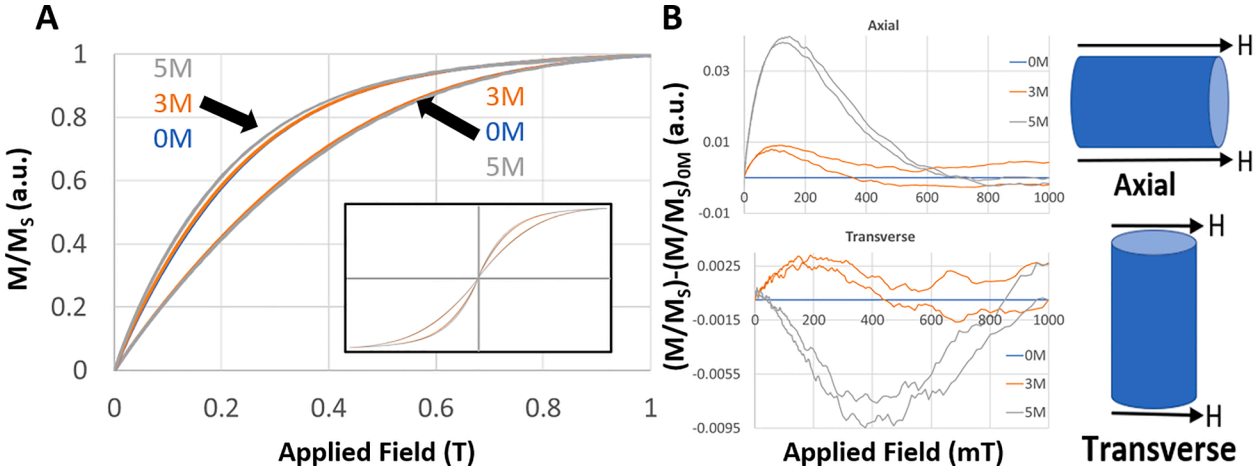

Fig. 3. (A) The first quadrant of the hysteresis loops for 0 M, 3 M, and 5 M magnetic fields in both the axial and transverse orientations. The full loops from +/- 1 T are shown in the lower right of the hysteresis graph and is coincident with the values from the main figure. (B) Orientations are shown by the inserts of magnetic field direction (as denoted by the arrow) in relation to filament orientation. Hysteresis loops of the three sample types after undergoing hysteresis subtraction by the 0 M hysteresis loop in the transverse (above) and axial (below) orientations to elucidate deviations from the 0 M samples.

the differences in the field profile present significantly influence the magnetic anisotropy of the final filament.

Trends within the magnetoactive data demonstrate similar trends of anisotropy in the magnetically annealed samples. As shown in Figs. 4 and 5, the magnetoactive angle of deformation exhibited little change below 0.2, and had a significant increase in its angle between 0.2 T and the maximum applied field (0.4 T). The change in the deformation angle occurred at lower applied fields and more suddenly (steeper slope) for the 5 M samples compared to the 0 M samples. We hypothesize that this increase in deformation angle at a given applied field arises from the greater magnetization (and thus, magnetic force) that arises at that applied field due to the increased anisotropy present, likely from increased chaining within the sample. Between the 3 M and 5 M samples, the 5 M samples display a greater magnetoactive response in all applied field strengths. The 3 M samples show a decrease in magnetoactive response compared to 0 M samples; this weakened performance suggests decreased anisotropy in the sample. It is important to note the 5 M samples were difficult to extrude and due to this, the usable 5 M samples were of lower quality. During extrusion if any slack was present in the system then the filament would become magnetically attracted to the face of the magnet holder and break. This resulted in inconsistent lengths of filament and few usable sections. A potential solution would be installing a sensor for the pulling system to automatically adjust to changing extrusion speeds from changes in internal pressure.

The application of magnetic annealing in the processing of filament is shown to be able to affect the performance of MRE's positively or negatively depending on the profile of the magnetic field used. In both the magnetic and magnetoactive properties, the 5 M samples had increased performance over 0 M, likely arising from both chaining and orientation effects of the internal particulate due to the magnetic annealing. This aligns with initial assumptions and literature in that magnetic annealing using a continuous field leads to increased MRE performance [6]. The 3 M samples, however, had similar magnetic properties and decreased magnetoactive properties relative to 0 M, thus demonstrating that magnetic annealing controls performance of MRE's based on the magnetic field profile used. The non-uniform field used in the 3 M samples likely leads to decreased overall anisotropy by interfering with the natural flow anisotropy created during extrusion and thus disrupting alignment. Drag forces in the polymer flow during the extrusion process and the non-spherical shape of the particulate create more alignment down the central axis and results in a natural anisotropy. [16,17] The non-uniform field may work against these drag forces and disperse particulate, leading to less performance in the 3 M samples compared to the 0 M samples. Meanwhile, the uniform field works along the direction of the drag forces resulting in increased alignment. We acknowledge that differences in the thickness and shape of filament can influence these results and hope that our use of multiple samples, error bars, and inspection of diameter consistency helps address this. The impact of thickness is difficult to quantify given an increased resistance to mechanical deflection, but also the likely increase in magnetic material present to promote greater deflection. A more rigorous controlled study of the effect of composite beam thickness on the magnetoactive properties would need to be carried out to more accurately address this issue. Initial optical microscopy has been conducted and shows changes in polymer morphology under different magnetic annealing fields, but further study of particle characteristics is required. Future considerations also include analyzing different magnet arrays, including linear Halbach alignment, to create magnetic fields with greater rotational forces. This work shows that not only can magnetic annealing enhance performance in MRE's, but it could also decrease performance in extruded geometries depending on the profile of the magnetic field used during magnetic annealing. This indicates that the field profile used in a magnetic annealing setup has large effects on the properties of the final MRE and must be carefully chosen to ensure performance is enhanced.

4. Conclusion

In conclusion, magnetic thermoplastic elastomer filament was magnetically annealed in an in-line system under different applied field profiles to find the greatest increase in its performance. It was observed that the uniform magnetic annealing field gives the largest increase in both magnetic susceptibility and magnetoactive response while the nonuniform magnetic field gives a decrease in both properties indicating that magnetic and mechanical factors are affected by the magnetic annealing field. The nonuniform field appears to interfere with natural anisotropy created from the extrusion process resulting in decreased anisotropy, whereas the uniform magnetic field is promising for creating enhanced anisotropy in extruded thermoplastic composites containing magnetic particles. This work shows that extruded thermoplastic magnetic elastomers compatible with FDM 3D printing can be created with

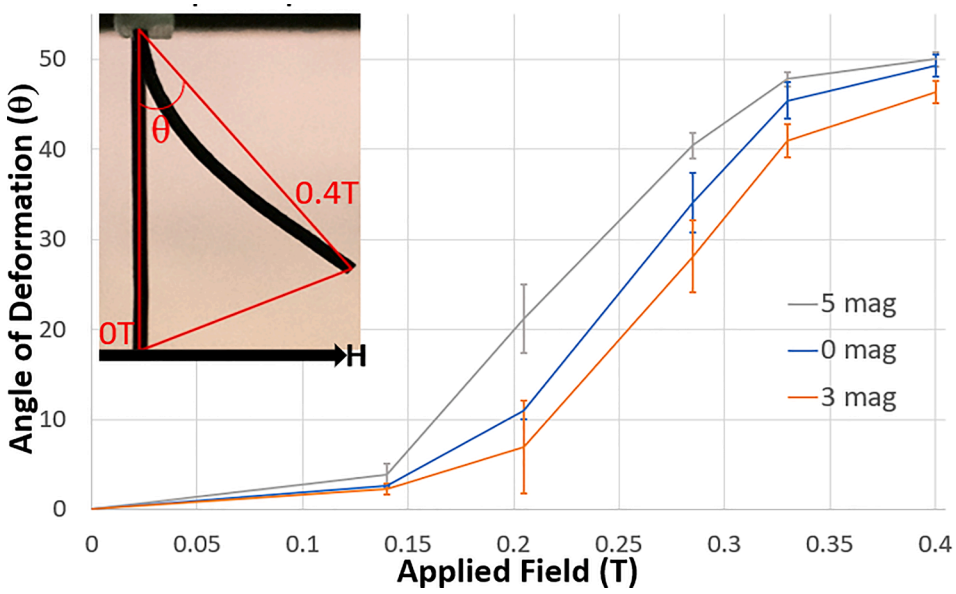

Fig. 4. Angles of deformation and standard error bars with three tests per sample type under a varied applied field. The inset shows an applied field image of a 0 M sample at both 0 T and 0.4 T with the resulting angle of deformation as shown by the red lines drawn onto the image. Direction of the applied field is denoted by the arrow below it labeled H. (For interpretation of the references to color in this figure legend, the reader is referred to the web version of this article.)

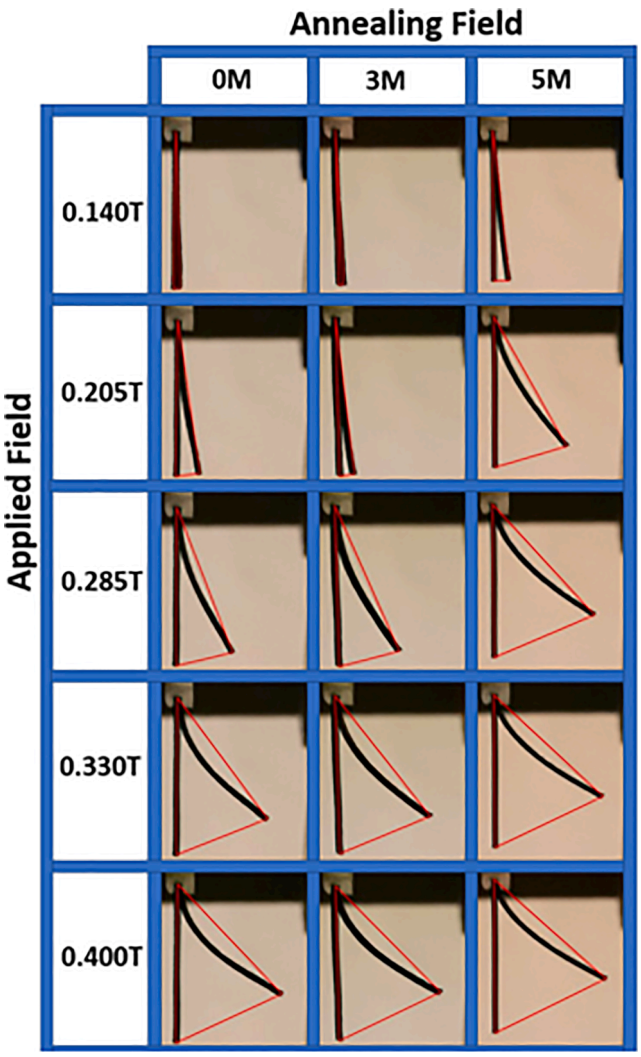

Fig. 5. Deformation of each sample type under increasing applied field along with an overlay of the sample at no applied field. Each sample used was cut to a length of 50 mm. Note: since each sample had the same saturation magnetization, the maximum deflections are similar; however, the sample responsiveness between 0.205 T and 0.330 T indicate magnetoactive properties of the annealed samples relative to the control.

an increased anisotropy, under certain magnetic field profiles, for greater overall performance and greater applicability in technologies. This work further highlights the importance of selecting and characterizing the magnetic field profile used in the magnetic annealing of extrusion field geometries.

CRediT authorship contribution statement

Nathan A. Fischer: Visualization, Investigation, Conceptualization. **Alex L. Robinson:** Investigation. **Thomas J. Lee:** Data curation, Software. **Thomas M. Calascione:** Investigation. **Lucas Koerner:** Software. **Brittany B. Nelson-Cheeseman:** Supervision, Resources.

Declaration of Competing Interest

The authors declare that they have no known competing financial interests or personal relationships that could have appeared to influence the work reported in this paper.

Acknowledgements

We would like to thank the Undergraduate Research Opportunities Program at the University of St. Thomas (UST) for partial funding of this project. We thank Professor Bill Robbins at the University of Minnesota (UMN) for assistance with magneto-mechanical data collection. We would also like to thank the Department of Physics at UST for use of their gaussmeter and multiaxial probe. Part of this work was performed at the Institute for Rock Magnetism (IRM) at UMN. The IRM is a US National Multi-user Facility supported through the Instrumentation and Facilities program of the National Science Foundation, Earth Sciences Division, and by funding from UMN.

References

[1] Ubaidillah, J. Sutrisno, A. Purwanto, S.A. Mazlan, Mazlan, Recent progress on magnetorheological solids: Materials, fabrication, testing, and applications, Adv. Eng. Mater. 17 (5) (2015) 563–597, https://doi.org/10.1002/adem.201400258.
[2] Z. Varga, G. Filipcsei, M. Zrínyi, Smart composites with controlled anisotropy, Polymer (Guildf) 46 (18) (2005) 7779–7787, https://doi.org/10.1016/j.polymer.2005.03.102.
[3] P.V. Lockette, S.E. Lofland, J. Biggs, J. Roche, J. Mineroff, M. Babcock, Investigating new symmetry classes in magnetorheological elastomers: Cantilever bending behavior, Smart Mater. Struct. 20 (10) (2011) 105022, https://doi.org/10.1088/0964-1726/20/10/105022.
[4] A. Munaz, M.J.A. Shiddiky, N.-T. Nguyen, Recent advances and current challenges in magnetophoresis based micro magnetofluidics, Biomicrofluidics. 12 (3) (2018) 031501, https://doi.org/10.1063/1.5035388.
[5] R.M. Erb, J.J. Martin, R. Soheilian, C. Pan, J.R. Barber, Actuating Soft Matter with Magnetic Torque, Adv. Funct. Mater. 26 (22) (2016) 3859–3880, https://doi.org/10.1002/adfm.201504699.
[6] Z. Varga, G. Filipcsei, M. Zrinya, Magnetic field sensitive functional elastomers with tuneable (sic) elastic modulus, Polymer 47 (2006) 227–233, https://doi.org/10.1016/j.polymer.2005.10.139.
[7] T.M. Calascione, N.A. Fischer, T.J. Lee, H.G. Thatcher, B.B. Nelson-Cheeseman, Controlling magnetic properties of 3D-printed magnetic elastomer structures via fused deposition modeling, AIP Adv 11 (2021) 25223, https://doi.org/10.1063/9.0000220.
[8] K. Gandha, L. Li, I.C. Nlebedim, B.K. Post, V. Kunc, B.C. Sales, J. Bell, M. P. Paranthaman, Manufacturing of anisotropic hybrid NdFeB-SmFeN nylon composite bonded magnets, J. Magn. Magn. Mater. (2018), https://doi.org/10.1016/j.jmmm.2018.07.021.
[9] R.M. Erb, R. Libanori, N. Rothfuchs, A.R. Studart, Composites reinforced in three dimensions by using low magnetic fields, Science 335 (6065) (2012) 199–204.
[10] Y. Kim, H. Yuk, R. Zhao, S.A. Chester, X. Zhao, Printing ferromagnetic domains for untethered fast-transforming soft materials, Nature 558 (7709) (2018) 274–279, https://doi.org/10.1038/s41586-018-0185-0.
[11] E.M. Palmero, D. Casaleiz, N.A. Jimenez, J. Rial, J. de Vicente, A. Nieto, R. Altimira, A. Bollero, Magnetic-polymer composites for bonding and 3d printing of permanent magnets, IEEE Trans. Magn. 55 (2) (2019) 1–4, https://doi.org/10.1109/TMAG.2018.2863560.
[12] A.H. Morgenstern, T.M. Calascione, N.A. Fischer, T.J. Lee, J.E. Wentz, B.B. Nelson-Cheeseman, Thermoplastic magnetic elastomer for fused filament fabrication, AIMS Mater. Sci. (2019), https://doi.org/10.3934/matersci.2019.3.363.
[13] C. Huber, S. Cano, I. Teliban, S. Schuschnigg, M. Groenefeld, D. Suess, Polymer-bonded anisotropic SrFe12O19 filaments for fused filament fabrication, J. Appl. Phys. 127 (6) (2020) 063904, https://doi.org/10.1063/1.5139493.
[14] T.J. Lee, A.H. Morgenstern, T.A. Höft, B.B. Nelson-Cheeseman, Dispersion of particulate in solvent cast magnetic thermoplastic polyurethane elastomer composites, AIMS Mater. Sci. (2019), https://doi.org/10.3934/matersci.2019.3.354.
[15] Technical Specifications: NinjaFlex® 3D Printing Filament. Available from: https://ninjatek.fppsites.com/wp-content/uploads/2018/10/NinjaFlex-TDS.pdf.
[16] C. Rauwendaal, Polymer Extrusion, in: C. Rauwendaal (Ed.), Polymer Extrusion, Carl Hanser Verlag GmbH & Co. KG, München, 2014, pp. I–XVI, https://doi.org/10.3139/9781569905395.fm.
[17] P. Butler, Shear induced structures and transformations in complex fluids, Curr. Opin. Colloid Interface Sci. 4 (3) (1999) 214–221, https://doi.org/10.1016/S1359-0294(99)00041-2.